Werk

Terms and Conditions

Contact

Niedersächsische Staats- und Universitätsbibliothek Göttingen
Georg-August-Universität Göttingen
Platz der Göttinger Sieben 1
37073 Göttingen
Germany
Email: gdz@sub.uni-goettingen.de

J. Geophys. 43, 375–388, 1977

Journal of Geophysics

Elastic Wave Propagation in a Highly Scattering Medium —A Diffusion Approach

A.M. Dainty* and M.N. Toksöz

Department of Earth and Planetary Sciences, Massachusetts Institute of Technology 24-414, 77 Massachusetts Ave., Cambridge, MA 02139, USA

Abstract. The principle of conservation of energy, in the form of the equation of radiative transfer, is used to treat the case of strong scattering of elastic waves. If the medium is isotropic, if all the energy present has been scattered many times, and if the time and distance scales of the problem are long compared to the time and distance scales of the scattering process, then the average flow of energy is described by the diffusion equation with an additional term representing linear dissipation to heat. Model seismic experiments using holes drilled in aluminum plates as scatterers confirm the applicability of the formalism. The diffusion formalism has been successfully applied to lunar seismograms and to some earth data. The results of studies of lunar seismograms show that the zone of strong scattering on the moon is confined to a near surface zone.

Key words: Elastic waves – Scattering – Diffusion – Ultrasonic models – Lunar seismology.

Introduction

In an elastic medium with a simple, deterministic structure, the transmission of energy within the medium may be described by the propagation of various types of elastic waves. The classical theory of seismology as applied to the earth uses this description. However, any real medium, such as the earth, contains many heterogeneities that can only be described in a statistical way. The effect of these heterogeneities is to produce a random, scattered wave field which must be included with the deterministic field in a complete description of the elastic energy distribution.

If the effect of the heterogeneities is small, the scattered field may be treated as a perturbation of the deterministic field (Chernov, 1960; Knopoff and

* To whom offprint requests should be sent

Hudson, 1964). In the earth, such is frequently the case (Aki, 1973; Cleary and Haddon, 1972; Aki and Chouet, 1975). The first seismograms returned from the moon, however, showed that conditions there were somewhat different from earth. Extremely small first arrivals were followed by a long, complex train of waves whose amplitude slowly increased to a maximum after several minutes and then gradually decayed over a period of an hour or more (Latham et al., 1970). The clear body phases and dispersed surface waves so characteristic of earth seismograms are not present, indicating that this coda consists of scattered waves. The extremely strong scattering this implies is due to the absence of water on the moon, which prevents cracks from annealing under moderate pressures. The long duration of the coda is due to low attenuation, again a result of the absence of water (Tittman et al., 1975).

To understand and model the lunar case of extremely strong scattering, some other formalism than the perturbation method is needed. A fruitful approach has been the use of the diffusion equation with linear dissipation (Nakamura et al., 1970; Berckhemer, 1970; Latham et al., 1970, 1972; Dainty et al., 1974; Toksöz et al., 1974; Nakamura, 1976; Wesley, 1965). In this paper we will first discuss the theoretical basis for the use of the diffusion equation, then the result of ultrasonic experiments designed to test the theory will be presented, and finally some mention will be made of the applications, both lunar and terrestrial, of the theory.

Theory

A situation is envisaged in which the effect of scattering is so strong that all energy is scattered energy. The acoustic case will be presented, and then the extension to the elastic case will be discussed. In our derivation the principle of conservation of energy is applied to the wave field, together with physical ideas about waves. The force equation usually used in elastic problems has not been solved for this case of strong scattering.

We regard the acoustic wave field as being made up of plane monochromatic waves of frequency f, travelling in all directions with random phases – thus, energies are additive, not amplitudes. If we define direction by polar angles θ, ϕ, and $e(\vec{R}, t, \theta, \phi)$ as the energy density at $\vec{R}, t$ of waves propagating in direction θ, ϕ, then

$$E(\vec{R}, t) = \int_s e(\vec{R}, t, \theta, \phi)\, d\omega$$

where $d\omega$ is an element of solid angle and the integration is over all solid angles. $E(\vec{R}, t)$ is the total energy density. We consider the medium through which the waves are propagating as having a wave velocity c, and ρ scatterers/unit volume. The scatterers each have a total scattering cross-section of σ and a differential scattering cross section $\Omega(\Theta)$, taken to be a function of scattering angle Θ only. Then

$$\sigma = \int_s \Omega(\Theta)\, d\omega.$$

Note that σ and Ω are generally strong functions of frequency. We consider an elemental volume δV, and waves travelling in direction θ, ϕ. Then the conservation of energy states:

$$\frac{\partial e}{\partial t}\delta V = -\int_{\Sigma} \vec{F}\cdot\vec{n}\, d\Sigma + \delta V\Big[\int_{s} \rho c\, e(\theta', \phi')\, \Omega(\Theta)\, d\omega' - \int_{s} \rho c e(\theta, \phi)\, \Omega(\Theta)\, d\omega' - a e\Big] \tag{1}$$

The first term on the right in (1) is the net flux across the surface Σ of δV, with normal $\vec{n}$, the second term represents energy scattered into direction θ, ϕ from all other directions θ', ϕ', the third term represents energy scattered out of θ, ϕ into all other directions, and the fourth term represents energy dissipated into heat. The dissipation constant $a = 2\pi f/Q$, where Q is the seismic quality factor. For the flux $\vec{F}$ we use the expression for a travelling wave,

$$\vec{F} = c\vec{k}e$$

where $\vec{k}$ is a unit vector in the direction of propagation of the wave.

Applying Gauss's theorem to the second term in (1), we obtain

$$\frac{\partial e}{\partial t} + \vec{V}\cdot c\vec{k}e + ae = \int_{s} \rho c\, \Omega(\Theta)\, [e(\theta', \phi') - e(\theta, \phi)]\, d\omega'. \tag{2}$$

This is the time-dependent equation of radiative transfer (Chandrasekhar, 1960). In deriving (1) and (2) we have assumed it is possible to define a volume δV sufficiently small that multiple scattering may be ignored within δV.

We next wish to parameterize the scattering medium in terms of a scale length. To do this, we consider a wave field consisting of a plane wave travelling in some particular direction θ_0, ϕ_0 at $t = 0$

$$e(\vec{R}, t, \theta, \phi) = \delta(\theta - \theta_0)\, \delta(\phi - \phi_0)\, e(\vec{R}, t) \quad \text{at } t = 0.$$

As time increases, energy will be scattered into other directions, and eventually, via multiple scattering, back into direction θ_0, ϕ_0. We shall, however, temporarily ignore this latter effect in deriving (4) below, i.e., we will ignore the first term in square brackets on the right hand side of (2). We will also ignore anelastic attenuation, and choose the x-axis of rectangular coordinates to lie along the direction θ_0, ϕ_0. (We will *not* ignore these two effects subsequent to Equation (4).) Then (2) becomes

$$\frac{\partial e}{\partial t} + c\frac{\partial e}{\partial x} = -\rho\sigma c e.$$

Using the Lagrangian relation $\frac{\partial}{\partial t} + c\frac{\partial}{\partial x} = c\frac{d}{ds}$ where s is distance travelled with

a particular wavefront, we have

$$\frac{de}{ds} = -\rho\sigma e$$

$$e = e_0 \cdot \exp(-\rho\sigma s) = e_0 \cdot \exp(-s/\lambda) \tag{3}$$

where

$$\lambda = 1/\rho\sigma = \text{mean free path.} \tag{4}$$

The mean free path defined above is the average distance energy travels before it is scattered, and is the characteristic scale length of the scattering process. In the formalism we will develop, all the complexities of the scattering medium are described by the parameter λ. This will only be possible if the time and distance scales over which the average energy density changes are long compared to λ/c and λ respectively. Since σ is a function of frequency, so is λ; λ may be greatly different for waves of different frequencies.

We return now to the case of a random wave field with energy travelling in all directions. The terms on the right hand side of Equation (2) represent the exchange of energy through the scattering process between waves travelling in various directions. If the scattering is strong, however, and a time long compared with λ/c has passed, a radiation balance will be set up such that

$$\int_s \Omega(\Theta)\,[e(\vec{R}, t, \theta', \phi') - e(\vec{R}, t, \theta, \phi)]\, d\omega' \to 0. \tag{5}$$

Relation (5) demands that all of the energy be scattered energy. Equation (2) may be further modified by noting that it is written in terms of $e(\vec{R}, t, \theta, \phi)$, which is not a measurable quantity if waves travelling in different directions cannot be separated. Integrating over all angles will yield $E(\vec{R}, t)$, which is measurable. Performing the integration

$$\frac{\partial E}{\partial t} + \vec{V} \cdot c \int_s \vec{k}\, e(\vec{R}, t, \theta, \phi)\, d\omega + aE = 0. \tag{6}$$

To evaluate the second integral in (6), additional assumptions must be made. We will assume that at any point in the medium, under the influence of strong scattering, radiation is isotropic to zeroth order. This is reasonable if all the energy is scattered energy, and if in addition the medium has no "grain", or preferred direction. Then

$$E(\vec{R}, t) = \int_s e(\vec{R}, t, \theta, \phi)\, d\omega = 4\pi e(\vec{R}, t). \tag{7}$$

However, since energy travels a finite distance λ before being scattered, the energy field cannot be completely isotropic unless the energy field is also homogeneous. If a gradient of energy is present, slightly more energy will come from the up gradient direction than from the down gradient direction, because there is more energy present at a distance λ in the up gradient direction. Using

(7), then, we write

$$e(\vec{R}, t, \theta, \phi) = \frac{1}{4\pi}\left(E(\vec{R}, t) + \lambda \vec{r} \cdot \vec{\nabla} E(\vec{R}, t)\right) \tag{8}$$

(8) states that the energy seen at $\vec{R}$ has come from the surface of a sphere of radius λ centered about $\vec{R}$. $\vec{r}$ in (8) is a unit vector from $\vec{R}$ pointing in the direction $180-\theta$, $180+\phi$. Thus $\vec{k} = -\vec{r}$. The remaining integral in (6) now becomes two integrals, the first of which is

$$-\frac{1}{4\pi}\int_s \vec{r} E(\vec{R}, t)\, d\omega = -\frac{E(\vec{R}, t)}{4\pi}\int_s \vec{r}\, d\omega = 0. \tag{9}$$

The second integral is

$$-\frac{\lambda}{4\pi}\int_s \vec{r}[\vec{r} \cdot \vec{\nabla} E(\vec{R}, t)]\, d\omega = -\frac{\lambda}{3}\vec{\nabla} E(\vec{R}, t). \tag{10}$$

(10) is most easily derived by setting up a rectangular coordinate system with one axis, x, say, along the direction of $\vec{\nabla} E(\vec{R}, t)$. Contributions along the y and z axes then cancel by symmetry in the integration over the sphere. Substituting (9) and (10) in (6) we obtain

$$\frac{\partial E}{\partial t} = \frac{c\lambda}{3}\nabla^2 E - aE. \tag{11}$$

The parameter $\frac{c\lambda}{3}$ will be written as ξ, and is known as the diffusivity. The parameter $a = 2\pi f/Q$, as previously stated; note that Q is in general a function of frequency. If different regions through which the energy travels have different Q's, the average of $1/Q$ weighted by the residence times in the various regions must be used (Wesley, 1965, Eq. (4)).

This derivation is similar to that used in the kinetic theory of gases (Jeans, 1925, p. 307–310). We have discussed the three-dimensional case. For the two-dimensional case, a similar discussion leads to

$$\xi = \frac{c\lambda}{2}. \tag{12}$$

The discussion above was for the acoustic case. In a homogeneous elastic medium, two types of waves, compressional and shear, exist. If there is strong scattering, however, the two types will be coupled, and if the coupling is strong enough they will be locked into a radiation balance which depends only on the properties of the scattering medium, provided that the time and distance scales of the problem are much longer than the corresponding scales for the scattering process. Thus the diffusion equation should still apply, provided the correct value of the diffusivity is used. Since the diffusivity is the coefficient of the flux term in (11), and since fluxes are additive and proportional to the energy, the

appropriate diffusivity to use is

$$\xi = R\xi_p + (1-R)\xi_s \tag{13}$$

where R is the proportion of the energy in compressional waves, ξ_p is the diffusivity calculated for compressional waves and ξ_s is the diffusivity calculated for S waves. It should be noted that, whilst the value of R depends on the nature of the scattering medium, it is expected to be typically 10% (Knopoff and Hudson, 1964), i.e., most of the scattered energy is in the form of S waves.

To solve Equation (11), note that writing $E = E_0 \exp(-at)$ yields the classical equation of heat transfer; a wide literature of solutions exists for this equation (see, for example, Carslaw and Jaeger, 1959). Since seismic pulses are very short relative to the time scale of the problems we shall consider, the Green's function for the appropriate boundary conditions is required. We emphasize again that (11) can only be applied to narrow band signals, since the scale parameter λ is in general a strong function of frequency.

The solutions of (11) as applied to special problems are given in the following sections.

Ultrasonic Model Experiments

To test the applicability of the diffusion formulation to seismic energy propagation in a highly scattering medium a set of ultrasonic model experiments were carried out in the laboratory (Dainty et al., 1974; Pines, 1973; Toksöz et al., 1974). These experiments used the propagation of ultrasonic pulses in plates with various densities of scatterers. The plates were 1/16″ aluminum and the scatterers consisted of either randomly distributed circular holes (with diameters smaller than the dominant wavelength) or grooves of random orientation. Scatterer densities, sizes and the width of the scattering region were varied in these experiments.

A schematic diagram of the experimental set-up is shown in Figure 1. A pulse of approximately 2 μs duration is generated by the pulse generator and applied to the plate by the source transducer. The receiver transducer is

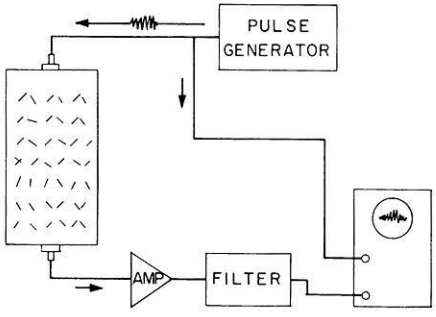

Fig. 1. Schematic diagram of ultrasonic model experiment

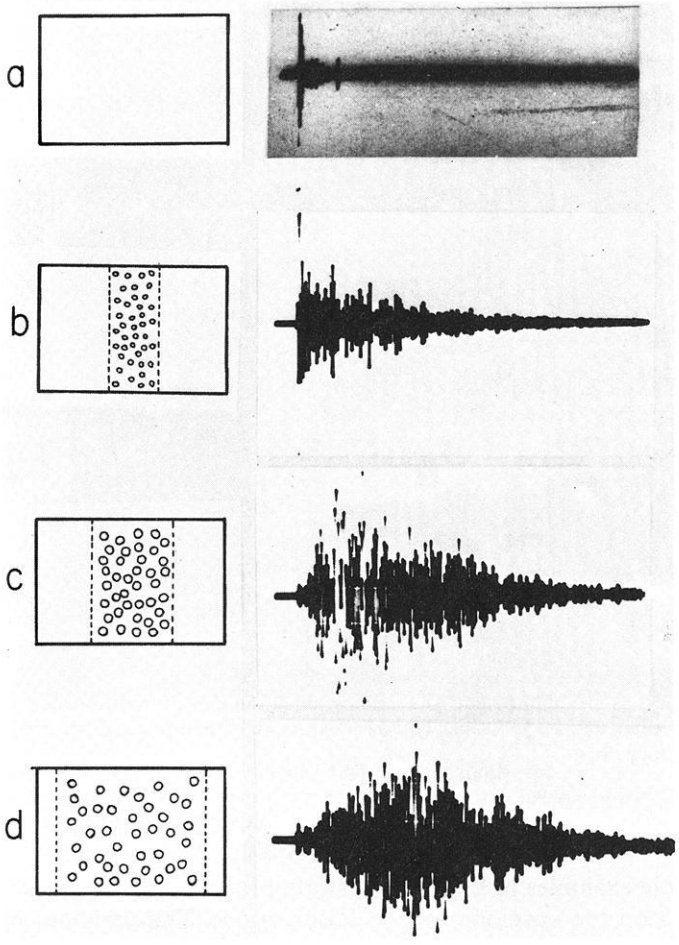

Fig. 2a–d. Ultrasonic model seismograms illustrating different amounts of scattering. The plates used are indicated schematically at the left of each seismogram. See text for discussion. Total length of each trace is 1 ms

mounted at the opposite end. The plate is approximately 25×80 cm. The scatterers may cover the whole or part of the plate. The edges of the plate are serrated and covered by absorbing modelling clay to minimize side reflections and surface waves.

Figure 2 shows seismograms generated by different scatterers at a fixed frequency of 330 khz. Without scatterers (Fig. 2a) the transmitted wave is pulse like. A few side reflections are visible since no clay or serrations were used in this case. In Figure 2b, c, d the successively increased effects of scattering are demonstrated. In Figure 2b, 243 scatterers (holes, 0.3 cm diameter) are distributed in the middle section of the plate over a 22 cm wide band, as illustrated on the right hand side. In Figure 2c, 243, 0.6 cm diameter scatterers are distributed over a 34-cm wide band. In Figure 2d, the same number of scatterers covers a

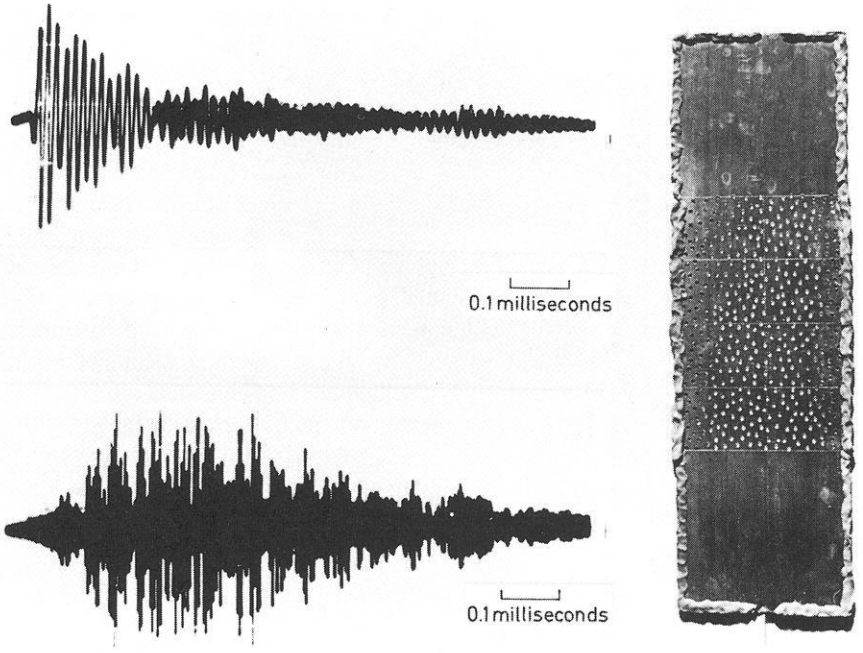

Fig. 3. Ultrasonic model seismograms illustrating the effects of different frequencies. The plate used to produce both seismograms is shown on the right. The seismogram at the top left was produced by using a band pass filter of center frequency 70 khz. The seismogram at bottom left was produced using a 330 khz center frequency filter

65 cm wide region. These examples in Figure 2 illustrate progressively the effects of increasing scattering on the envelopes of the seismograms. The variables in these cases are the density of the scatterers, the width of the scattering zone, and the size of the scatterers.

Another experiment examined the wavelength dependence of scattering. This is illustrated in Figure 3, where the photograph of the plate used is shown on the right. Seismograms, narrow band-pass filtered at center frequencies $f_0 = 70$ khz and $f_0 = 330$ khz are shown on the right. Note that high frequency waves are scattered more extensively because of the greater scattering efficiency of the holes for the shorter wavelength, and the resulting shorter mean free path.

To quantitatively compare the experimental results with the theoretical predictions, described in the previous section, a set of measurements were made varying only one parameter. Four plates, each 24 cm wide and with 0.6 cm diameter holes were used. The density of scatterers was 0.56 holes/cm^2. This corresponds to a diffusivity $\xi = 4 \times 10^5$ cm^2/s. The plate velocity of shear waves is $c = 3.2$ mm/μs. The width of the scattering band in the four experiments was $u = 4.5$, 9, 18 and 36 cm. The seismograms are shown in Figure 4.

A theoretical solution for the diffusion of energy from a point impulse applied to the edge of a two dimensional rectangular plate, under the boundary

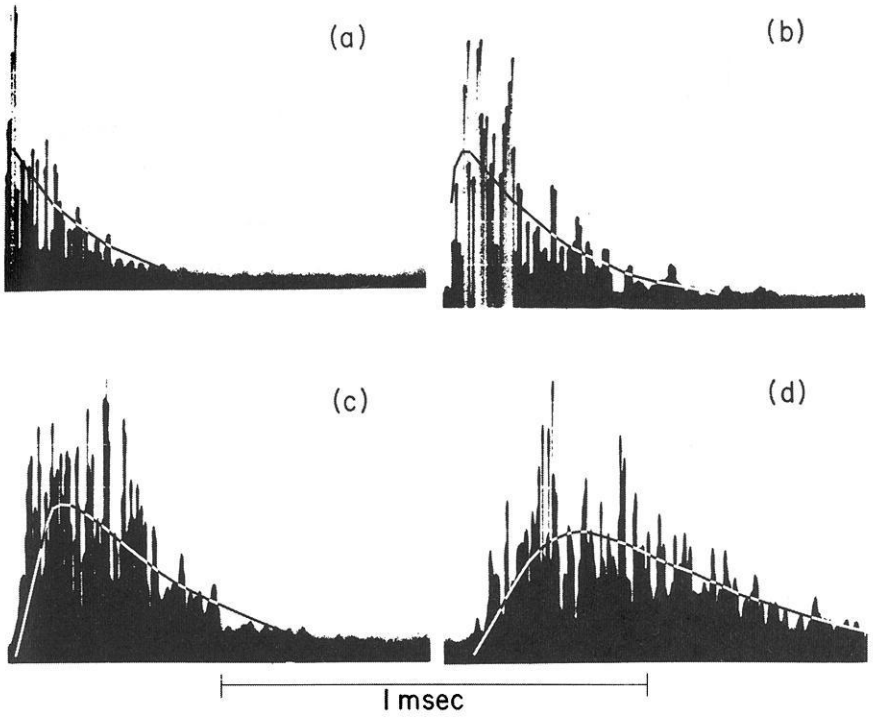

Fig. 4. Comparison of ultrasonic model seismograms and diffusion theory. The seismograms are similar to those shown previously but have been cut in half along the line of zero displacement. The smooth curves are theoretical fits. See text for discussion. From Toksöz et al. (1974)

condition that no energy may escape from the plate is given by (Carslaw and Jaeger, 1959, p. 360);

$$E=\frac{e^{-at}}{uv}\left[1+2\sum_{n=1}^{\infty}\cos\left(\frac{n\pi x}{u}\right)\cos\left(\frac{n\pi x'}{u}\right)\exp\left(-\xi n^2\pi^2 t/u^2\right)\right]$$
$$\cdot\left[1+2\sum_{n=1}^{\infty}\cos\left(\frac{n\pi y}{v}\right)\cos\left(\frac{n\pi y'}{v}\right)\exp\left(-\xi n^2\pi^2 t/v^2\right)\right]. \tag{14}$$

In (14) x, y is the field point, x', y' the source point. The plate is defined by $0\leqq x\leqq u$, $0\leqq y\leqq v$. In our example, the transmitting and receiving transducers are mounted in the center of opposite edges of the plate, i.e. $x=u$, $y=v/2$, $x'=0$, $y'=v/2$, and (14) becomes (Toksöz et al., 1974):

$$E(u,v,t)=\frac{e^{-at}}{uv}\left[1+2\sum_{n=1}^{\infty}(-1)^n\exp\left(-\xi n^2\pi^2 t/u^2\right)\right]$$
$$\cdot\left[1+2\sum_{n=1}^{\infty}\exp\left(-4\xi n^2\pi^2 t/v^2\right)\right]. \tag{15}$$

The theoretical curves in Figure 4 were calculated using Equation (15) (taking the square root of energy for amplitude) with parameters $v=24$ cm, $\xi=4\times10^5$ cm^2/s, a Q value of 70 and the appropriate u values (4.5, 9, 18 and 36 cm). The agreement between the theory and the laboratory results is good. A question might arise regarding the relatively low Q value (70) that was used in the theoretical fit; Q in aluminum is much higher ($Q_{al}\geqq1000$). The lowering of the Q value is due primarily to absorption in the clay around the edges of plate.

These laboratory experiments and the comparison shown in Figure 4a, b, c, d demonstrate the applicability of the diffusion equation to seismic energy propagation in a highly scattering medium.

Seismological Applications of the Theory

The major application of diffusion theory in seismology has been the lunar case, with occasional use in terrestrial seismology. As mentioned previously, the importance of scattered energy on the moon relative to the earth is due in large part to the total absence of water in the lunar near-surface environment. This absence means that cracks and fractures in the near surface zone will not anneal as they do on earth – a situation that is reinforced by the low lunar pressure gradient with depth and cooler temperature in the lunar interior relative to earth. Since the lunar surface has been bombarded with meteorites throughout its history, cracks and fractures are expected. Another important effect of the lack of water and other volatiles is the extremely high values of the seismic quality factor Q (Tittman et al., 1975) in the lunar environment. This means that energy scattered many times and travelling long paths to the seismometer may be detected.

In the application of diffusion theory to the moon, an early result was the finding that strong scattering is limited to the near-surface region (Latham et al., 1971). This leads to three different types of scattered coda: for close surface events, where the source receiver distance is not too large, the dominant transmission of seismic energy is by horizontal diffusion through the scattering zone. For far surface events, energy diffuses through the near-surface scattering zone into the deeper regions of the moon where it propagates without scattering and then diffuses back up to the receiver. For events occurring deep within the moon, the scattering layer is traversed once by energy en route to the surface. These relations are illustrated in Figure 5.

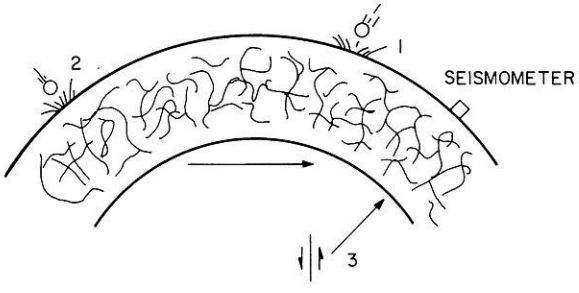

Fig. 5. The scattering zone on the moon and possible wave paths. Situation 1 is close impact, 2 far impact, and 3 moonquake. From Dainty et al. (1974)

Since the scattering zone is confined near the surface, it is modelled by a diffusing layer over a half space within which seismic energy propagates as waves without scattering.

The solution of (11) for an anisotropically diffusing layer over a half-space has been given by Dainty et al. (1974). In their treatment, the diffusivities in the vertical direction (ξ_v) and the horizontal direction (ξ_H) are different, to model the vertical heteorgeneity commonly found in nature. The solution for a point impulse at the origin of cylindrical coordinates r, z, is

$$E=\frac{1}{4\pi\xi_H t h}\exp\left[-\frac{r^2}{4\xi_H t}-at\right]\sum_{n=1}^{\infty}\frac{b_n\cos(b_n z/h)}{2b_n+\sin 2b_n}\exp\left[\frac{-t\xi_v b_n^2}{n^2}\right] \tag{16}$$

where the b_n are the positive roots of

$$b\cdot\tan b=\frac{hV}{\xi_v} \tag{17}$$

starting with the numerically smallest. h is the thickness of the layer, and V is the velocity of propagation of waves in the half-space. Note in (17) that if the right hand side is large, then the low order b_n are not a strong function of V; the low order terms are the ones which will dominate in (16) for large t. From (16) and the principle of reciprocity we may also derive the case of a plane impulsive source on either surface of the layer as observed at the other surface by integrating over all r:

$$E=[4/h]\,e^{-at}\sum_{n=1}^{\infty}\frac{b_n\cos b_n}{2b_n+\sin 2b_n}\exp\left[-\frac{t\xi_v b_n^2}{h^2}\right]. \tag{18}$$

To compare the diffusion formalism, which refers to seismic energy in a narrow frequency band, with lunar seismograms, we form the energy envelope of the seismograms by Fourier transforming a moving window 51.2 s long over the seismogram to obtain the power spectrum and plotting the power in a narrow band as a function of time. This envelope may be compared directly with Equations (16) and (18). An example of this comparison is shown in Figure 6, which uses data from two close-in artificial impacts on the moon (Toksöz et al., 1974). The fits shown from Equation (16) use $\xi_H=2\,\mathrm{km}^2/\mathrm{s}$, implying a mean free path of between 1 and 10 km, depending on the wave velocity used. The thickness of the surface scattering zone is between 1 and 20 km (Toksöz et al., 1974). Q is 5000.

The example in Figure 6 is for a close surface event. If we assume that the effect of scattering near the source is the same as scattering near the receiver, and if the time spent in the non-scattering interior of the moon is short compared with the time spent in the scattering zone, then there is a convolutional relationship (Dainty et al., 1974) between the energy envelope $f(t)$ of the far surface events and the energy envelope $m(t)$ of deep focus events, namely:

$$f(t)=A\cdot m(t)^* m(t) \tag{19}$$

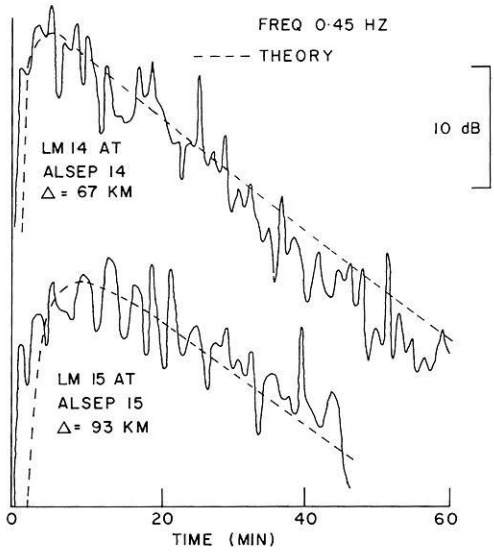

Fig. 6. Close impact energy envelopes (solid curves) and theoretical fits (dashed curves) for the Apollo 14 lunar module impact received at Alsep station 14 and the Apollo 15 lunar module impact received at Alsep station 15. The graph is a semilog plot, the ordinate being energy on a decibel scale with an arbitrary reference level. The envelopes have been separated for clarity. From Toksöz et al. (1974)

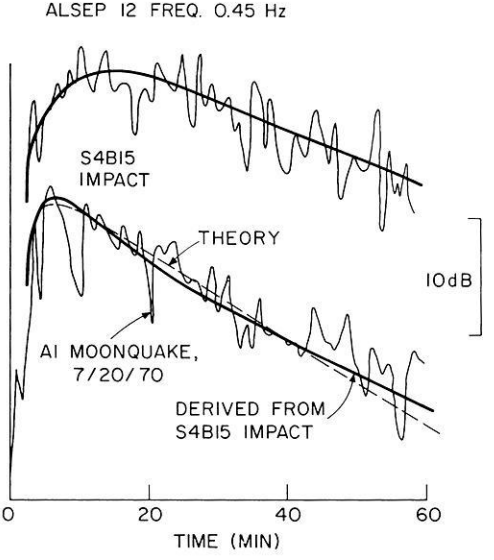

Fig. 7. Comparison of far impact and deep focus moonquake energy envelopes. Top, Saturn 4 Booster impact as received at Alsep station 12, light curve. The heavy curve in the top half is a smooth curve drawn through the data. The heavy curve in the bottom half of the figure is derived from this line using (19). The light curve in the bottom half of the figure is the energy envelope for an Al moonquake, and the dashed curve is a theoretical fit. From Dainty et al. (1974)

where A is a multiplicative constant which depends on range and * indicates convolution: (19) is illustrated in Figure 7, which shows envelopes for a far impact and a deep focus moonquake. Two theoretical fits to the deep focus energy envelope are shown – one derived from the far impact envelope using (19), one a theoretical fit using (18) and the same model as for Figure 6.

Diffusion theory has also been applied to the coda of local earthquakes (Aki and Chouet, 1975, with references to earlier work). These authors find that at frequencies around 1 Hz most of the coda is scattered surface waves, whilst at frequencies of about 10 Hz and higher scattered body waves predominate. The mean free path for 1 Hz energy (surface waves) was comparable to that found on the moon but the mean free path at 10 Hz (body waves) was at least an order of magnitude larger. Q was much lower (100–1000) than the lunar case, reflecting the presence of water.

Conclusions

In the case of strong scattering of seismic waves, the average energy density as a function of time and space may be described by the diffusion equation with linear dissipation, provided that all the energy present has been scattered many times, and the time and distance scale of the problem are long compared to the scales that correspond to the scattering process. Ultrasonic experiments in the laboratory confirm the applicability of the formalism. The theory may be used to explain the characteristics of seismograms returned from the moon. In certain cases the theory may also be used to explain seismic observations on the earth, particularly the high frequency coda of local earthquakes.

Acknowledgements. Jacques Pines performed the ultrasonic experiments. We discussed our results with Keiiti Aki, Hans Berckhemer, Bernard Chouet, Peter Malin, Yosio Nakamura and Robert Phinney. This research was supported under NASA Grant NAS9-12334.

References

Aki, K.: Scattering of P waves under the Montana Lasa. J. Geophys. Res. **78**, 1334–1346, 1973

Aki, K., Chouet, B.: Origin of coda waves: source, attenuation and scattering effects. J. Geophys. Res. **80**, 3322–3342, 1975

Berckhemer, H.: A possible scattering mechanism for lunar seismic waves. Z. Geophys. **36**, 523–529, 1970

Carslaw, H.S., Jaeger, J.C.: Conduction of heat in solids, 2nd ed. London: Oxford University Press 1959

Chandrasekhar, S.: Radiative transfer. New York: Dover 1960

Chernov, L.A.: Wave propagation in a random medium. New York: McGraw-Hill 1960

Cleary, J.R., Haddon, R.A.W.: Seismic wave scattering near the core-mantle boundary: a new interpretation of precursors to PKIKP. Nature **240**, 549–550, 1972

Dainty, A.M., Toksöz, M.N., Anderson, K.R., Pines, P.J., Nakamura, Y., Latham, G.: Seismic scattering and shallow structure of the moon in Oceanus Procellarum. The Moon **9**, 11–29, 1974

Jeans, J.H.: The dynamical theory of gases, 4th ed. London: Cambridge University Press 1925

Knopoff, L., Hudson, J.A.: Scattering of elastic waves by small inhomogeneities. J. Acoust. Soc. Am. **36**, 338–345, 1964

Latham, G.V., Ewing, M., Press, F., Sutton, G., Dorman, J., Nakamura, Y., Toksöz, N., Wiggins, R., Derr, J., Duennebier, F.: Passive seismic experiment. Science **167**, 435–457, 1970

Latham, G.V., Ewing, M., Press, F., Sutton, G., Dorman, J., Nakamura, Y., Toksöz, N., Duennebier, F., Lammlein, D.: Passive seismic experiment, Apollo 14 Preliminary Science Report. NASA SP-**272**, 133–161, 1971

Latham, G.V., Ewing, M., Press, F., Sutton, G., Dorman, J., Nakamura, Y., Toksöz, N., Lammlein, D., Duennebier, F.: Passive seismic experiment, Apollo 16 Preliminary Science Report. NASA SP-**315**, Section 9, 1972

Nakamura, Y.: Seismic energy transmission in the lunar surface zone determined from signals generated by movement of lunar rover. Bull. Seism. Soc. Amer. **66**, 593–606, 1976

Nakamura, Y., Latham, G.V., Ewing, M., Dorman, J.: Lunar seismic energy transmission. EOS **51**, 776 (abs.), 1970

Pines, P.J.: Model seismic studies of intensely scattering media. M.Sc. Thesis, MIT 1973

Tittman, B.R., Curnow, J.M., Housely, R.M.: Internal friction quality factor $Q \geqq 3100$ achieved in lunar rock 70215, 85, Proc. Sixth Lunar Sci. Conf., Vol. 3, pp. 3217–3226. New York: Pergamon Press 1975

Toksöz, M.N., Dainty, A.M., Solomon, S.C., Anderson, K.R.: Structure of the moon. Rev. Geophys. Space Phys. **12**, 539–567, 1974

Wesley, J.P.: Diffusion of seismic energy in the near range. J. Geophys. Res. **70**, 5099–5106, 1965

Received November 29, 1976; Revised Version January 24, 1977